

16. Corefield, R. M. and Carlidge, J. E., Oceanographic and climatic implications of the Paleocene carbon isotope maximum. *Terra Nova*, 1992, **4**, 443–455.
17. Kumar, K. and Loyal, R. S., Eocene ichthyofauna from the Subathu Formation, northwestern Himalaya, India. *J. Palaeontol. Soc. India*, 1987, **32**, 60–84.
18. Samanta, B. K., Early Tertiary stratigraphy of the area around Garampani, Mikir, North Cachher Hills, Assam. *J. Geol. Soc. India*, 1971, **12**, 318–327.
19. Whiso, K., Ramesh, P., Venkatachalapathy, R. and Kachhara, R. P., Occurrence and age significance of *Planorotalites palmerae* (Cushman & Bermudez) in the Dillai Parbat area of Assam, NE India. In *Micropaleontology: Application in Stratigraphy and Paleooceanography* (ed. Sinha, D. K.), Narosa Publishing House, New Delhi, 2003, pp. 141–144.
20. Prasad, B. and Dey, A. K., The occurrence of Eocene sediments in Arunachal Pradesh: a palynological evidence. *Bull. ONGC*, 1986, **23**, 67–74.
21. Singh, T. and Singh, P., Late early Eocene larger foraminiferids from Siang district, Arunachal Pradesh, India and their significance. *Geosci. J.*, 1983, **4**, 141–156.
22. Lokho, K., Venkatachalapathy, R. and Raju, D. S. N., Uvigerinids and associated foraminifera and their value as direct evidence for shelf and deep marine paleoenvironments during Upper Dishang of Nagaland, Eastern Himalaya and implication in hydrogen exploration. *Indian J. Petrol. Geol.*, 2004, **13**, 1–7.
23. Lokho, K., Venkatachalapathy, R. and Raju, D. S. N., Stratigraphic tables for Northeast basins of India: with brief notes. *Indian J. Petrol. Geol.*, 2004, **13**, 79–96.
24. Lokho, K. and Prasad, K., Fossil pteropods (Thecosomata, holoplanktonic Mollusca) from the Eocene of Assam–Arakan basin, northeastern India. *Curr. Sci.*, 2008, **94**, 647–652.
25. Tewari, V. C., Sial, A. N., Kumar, K., Lokho, K. and Siddaiah, N. S., Late Cretaceous–Paleocene sedimentation, carbon isotope chemostratigraphy and basis evolution in the South Shillong Plateau. In *Seminar on Indo-Myanmar Ranges in the Tectonic Framework of the Himalaya and Southeast Asia*, Manipur University, Imphal, Abstract, 2008, pp. 52–54.
26. Lokho, K. and Raju, D. S. N., Recent biostratigraphic findings in the Assam–Arakan basins, NE India and their significance. In *Seminar on Indo-Myanmar Ranges in the Tectonic Framework of the Himalaya and Southeast Asia*, Manipur University, Imphal, Abstract, 2008, pp. 60–61.
27. Sahni, A. and Prasad, G. V. R., Geodynamic evolution of the Indian Plate: consequences for dispersal and distribution of biota. *Mem. Geol. Soc. India*, 2008, **66**, 203–225.
28. Tewari, V. C., Lokho, K., Kumar, K. and Siddaiah, N. S., Early foreland (Late Cretaceous–Paleocene) basin architecture and evolution of the Shillong shelf sedimentation, Meghalaya, Northeast India. In *The Forty Sixth Annual Convention and Meeting on Evolution of Himalayan Foreland Basin and Emerging Challenges*, Wadia Institute of Himalayan Geology, Dehradun, Abstract, 2009, pp. 44–45.

**ACKNOWLEDGEMENTS.** We are grateful to Prof. A. N. Sial, NEGLABISE Department of Geology, Federal University of Pernambuco, Recife, Brazil, for isotopic analysis of the Lakadong Limestone from Meghalaya. V.C.T.'s discussions on Tethyan Paleogene foraminifera and calcareous algae with Prof. Katia Drobne (Slovenia) and Prof. N. Pugliese, Drs Romana Melis and Roberta Romano, DisGam, University of Trieste, Italy, have been very fruitful. We thank Prof. B. R. Arora, Director, Wadia Institute of Himalayan Geology, Dehradun for facilities and permission to publish the paper. We also thank the authorities of the Mawmluch-Cherra Cement Ltd for the permission to sample in the Limestone Quarry.

Received 19 March 2009; revised accepted 23 November 2009

## Stream profiles as indicator of active tectonic deformation along the Intra-Foreland Thrust, Nahan Salient, NW India

Tejpal Singh<sup>1,2,\*</sup> and A. K. Awasthi<sup>1</sup>

<sup>1</sup>Department of Earth Sciences, Indian Institute of Technology Roorkee, Roorkee 247 667, India

<sup>2</sup>Present address: CSIR Centre for Mathematical Modelling and Computer Simulation, NAL Belur Campus, Bangalore 560 017, India

**Stream profiles along five major streams from the Nahan Salient in the Western Sub-Himalaya were investigated with special emphasis on reactivation/active tectonics of the Intra-Foreland Thrust (IFT). Each of the stream profiles is observed to consist of two to three segments of different stream gradients. Each segment comprises a 'stream reach' and is marked by a distinct stream-length (SL) gradient index. SL index curves drawn for the five streams show anomalous increase in its values at the contact of two stream reaches. These distinct anomalies are found associated with the surface exposure of IFT in the field. Likewise low mountain front sinuosity (1.1 to 2.4) and low valley width to height ratios (0.1 to 0.33) also reflect active tectonic deformation along the IFT due to reactivation. The present stream profile approach is simpler, easier and faster to locate sites of fault related reactivation.**

**Keywords:** Intra-Foreland Thrust, Nahan Salient, reactivation, stream long profiles, SL value.

THE Sub-Himalayan belt in the NW India is marked by the sinuous trace of the Main Boundary Thrust (MBT) giving rise to areas that are concave towards the foreland, known as reentrants, and areas that are convex towards the foreland, known as salients. The present study was carried out in the largest salient of NW India, i.e. the Nahan Salient (Figure 1). The Nahan Salient is located in between the Kangra and the Dehradun reentrants lying in its northwest and southeast respectively. The salient and the reentrants are marked by thrusts running parallel to sub-parallel to the Himalayan Frontal Thrust (HFT) in the NW–SE direction.

It is commonly believed that the Himalayan front has sequentially migrated southwards giving rise to new thrusts<sup>1–3</sup>. It is also believed that the newly formed thrusts are the focus of tectonic convergence as seen in the case of HFT at a number of places, all along its strike<sup>4–6</sup>. Consequently, many or almost all of the thrusts/faults that lie to the north of the HFT may have, at some time in the geological past, ceased to absorb the convergence of the Indian and Eurasian plates and were rendered inactive. In

\*For correspondence. (e-mail: geotejpal@yahoo.co.in)

such a scenario, any active tectonic deformation recorded along a fault north of the HFT, seems to be the result of its reactivation during the recent past. Here we focus on the active tectonic deformation along an IFT, also referred as the Nahan Thrust<sup>9</sup>, that lies between the MBT and HFT within the Nahan Salient. The IFT brings the older Lower Siwalik sandstone–claystone sequence over the younger Upper Siwalik sequence which is coarsening upward with sandy facies at the base and conglomeratic facies towards the top<sup>10</sup>.

This type of tectonic deformation is usually manifested by a change in drainage system which adjusts to the change in topographic slope gradient by changing its course<sup>7,8</sup>. Singh and Viridi<sup>9</sup> have brought to light some key topographic manifestations of such active tectonic deformation in the Nahan Salient just north of the HFT. These manifestations are represented by a break in topographic slope, steep valley walls in the hanging wall block, unstable slopes and low values of mountain front sinuosity. A good spatial correlation between these topographic features and the map trace of IFT has been documented<sup>9</sup>. The change in topographic slope brought about by the reactivation of IFT has also affected the stream pattern across the IFT<sup>9</sup>. However, no study has been carried out to understand the effect of this change in topographic slope on the behaviour and gradient of streams.

The present study was carried out using the drainage network from the Survey of India (SOI) topographic

maps and satellite imagery (IRS-1D LISS-III, path-95 row-49 procured on 28 February 2003) of the Nahan Salient. The two data set were georeferenced/rectified in the same coordinate system (Projection: Geographic lat./long., Spheroid: Everest and Datum: Everest) so that they could be spatially interfaced. Interestingly, a good correspondence between the drainage lines on the satellite imagery and that on the topographic maps was found. A total of five watersheds, enclosing the IFT were delineated from the topographic map based on the contours. The watershed boundaries correspond well with the topographic highs visible on the satellite imagery (Figure 2). Further, the main streams of each of the watersheds were digitized from the topographic map. Each of the digitized streams was visually verified for their spatial correspondence with those seen on the satellite imagery (Figure 2). The longest stream from each of the five watersheds was used to generate the stream profiles. Stream profiles are usually characterized by variation in the gradient, i.e. change in elevation ( $dH$ ) per unit length ( $dL$ ) of the stream. Such profiles have been extensively used for identification of anomalous zones, manifested by a sharp change in the stream gradient, along the stream course<sup>11,12</sup>.

In the present study, channel elevation ( $H$ ) was plotted against stream length ( $\log L$ ) (Figure 3). The semi-logarithmic plot of stream profile known as 'Hack profile', is not a straight line in form, rather each of these profiles consist of a number of straight line segments each of which is referred as a 'stream reach'. The number of stream reaches for each of the profiles varies from two to three (Figure 3). The stream reaches were identified by statistically fitting straight lines to the stream profile curves. Each of the stream reaches identified in this way is characterized by a particular stream gradient ( $K$ ). The

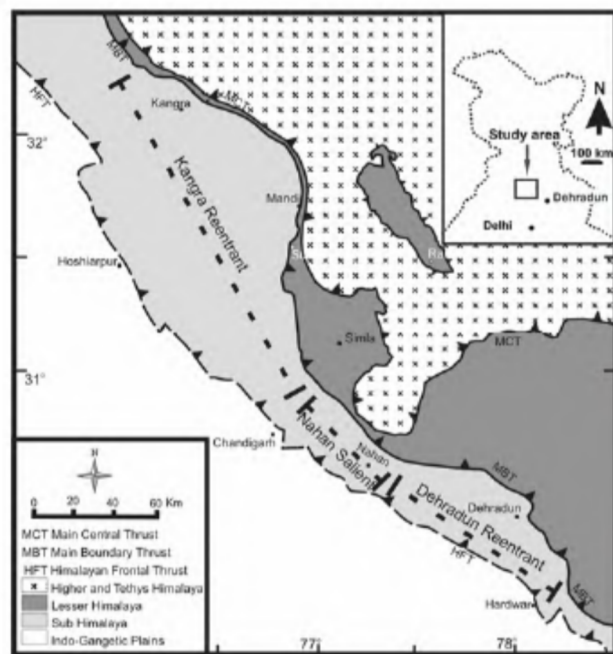


**Figure 1.** Tectonic sub-divisions of the NW Himalaya marked by the presence of the Kangra and Dehradun reentrants and Nahan Salient. The study area is located in the Sub-Himalayan belt of the Nahan Salient (see inset for geographical location).

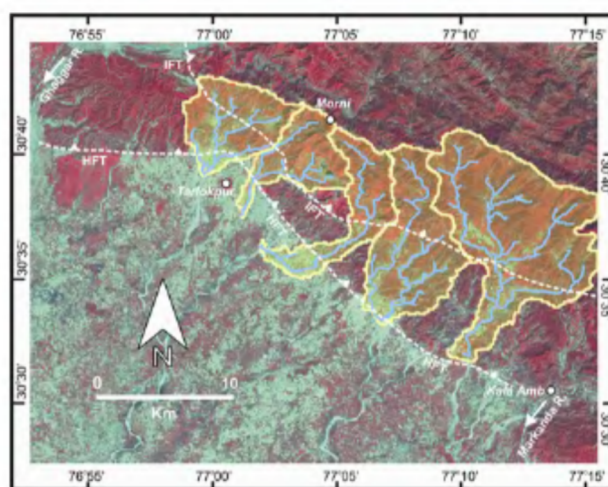


**Figure 2.** Watersheds and drainage lines delineated from the SOI topographic map correspond well with the ones seen on the satellite imagery. The watersheds are referred as Basin I through Basin V, from east to west. The HFT and IFT are marked by dotted lines for better visibility.

stream gradient ( $K$ ) can be worked out for each of the identified reaches in the five stream profiles as follows. Hack<sup>11</sup> gave the following relationship between elevation

( $H$ ) and distance from the source ( $L$ ) of a particular stream reach:

$$H = C - K \ln L, \quad (1)$$

where  $K$  is the slope of the straight line representing the stream reach profile (Figure 3) and is also known as the stream gradient index and  $C$  is a constant.

Likewise, the channel slope ( $S$ ) for a particular channel reach is obtained by differentiating  $H$  with respect to  $L$ . Hence, differentiating eq. (1) with respect to  $L$  gives the following relationships between  $S$  and  $K$ .

$$S = dH/dL = -K(1/L), \quad (2)$$

$$\text{or } K = -SL, \quad (3)$$

where the negative symbol indicates the direction of slope of the profile.

In other words,  $K$  value represents the product of slope and length of a stream reach, also known as the stream length gradient ( $SL$ ) index<sup>11</sup>. In a hilly terrain like the one under discussion, with appreciable slope and ephemeral drainage, the stream power is mainly a function of topographic slope ( $S$ ) and the upstream length ( $L$ ) of the stream reach. The  $SL$  index appropriately expresses stream power by representing the stream discharge through its length  $L$ . Hence, the  $SL$  index also characterizes stream power for a reach or an entire stream profile<sup>13,14</sup>.

All the five stream profiles from the Nahana Salient show a clear break in the stream gradient marked by an anomalous increase in the  $SL$  index (Figure 3). In the field, the anomalous increase in the  $SL$  index is observed to correspond with fault zones along all the stream profiles. Such breaks in the stream gradient and anomalous increase in the  $SL$  index are often marked by faults/fault zones<sup>11-14</sup>. By analogy to the works<sup>11-14</sup>, and the observations in the present study that are traceable laterally along the strike of the exposed IFT, it is inferred that stream profiles have been affected by tectonic reactivation along the IFT.

Steepening of the topographic slope due to the reactivation of the IFT increased the gradient of the streams cutting across the IFT, thereby causing severe downcutting in the hanging wall block, especially in the parts where the stream channels have low valley width to height ratios that range from 0.1 to 0.33 (ref. 9). Increased downcutting flooded the downstream channels with excess sediment load. Low load carrying competence of streams in relatively low stream gradient in the footwall block led to the debouching of sediments giving rise to braided channels (Figure 4). At the same time, vertical incision in the hanging wall block does not allow the retreat of the topographic front produced by reactivation thereby maintaining low values of the mountain front sinuosity that range from 1.1 to 2.4 (ref. 9).

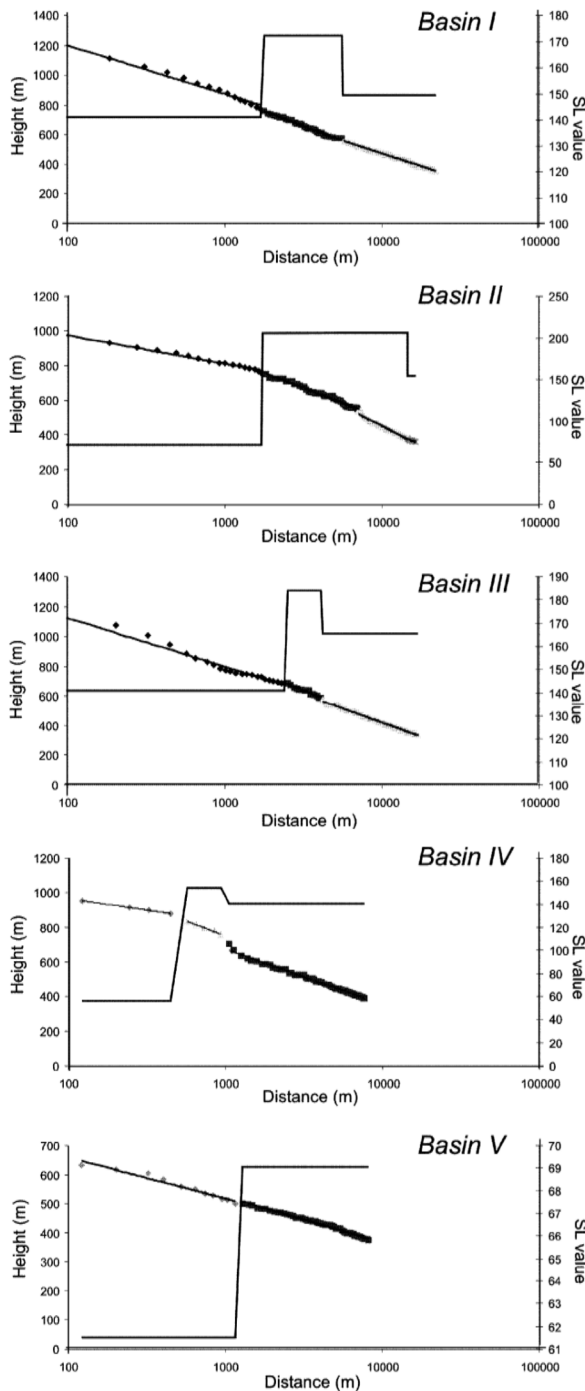


**Figure 3.** Stream profiles with different reaches and their respective  $SL$  indices (stepped curve). The break in stream profiles is clearly manifested by an increase in the  $SL$  index across the active thrust fault.



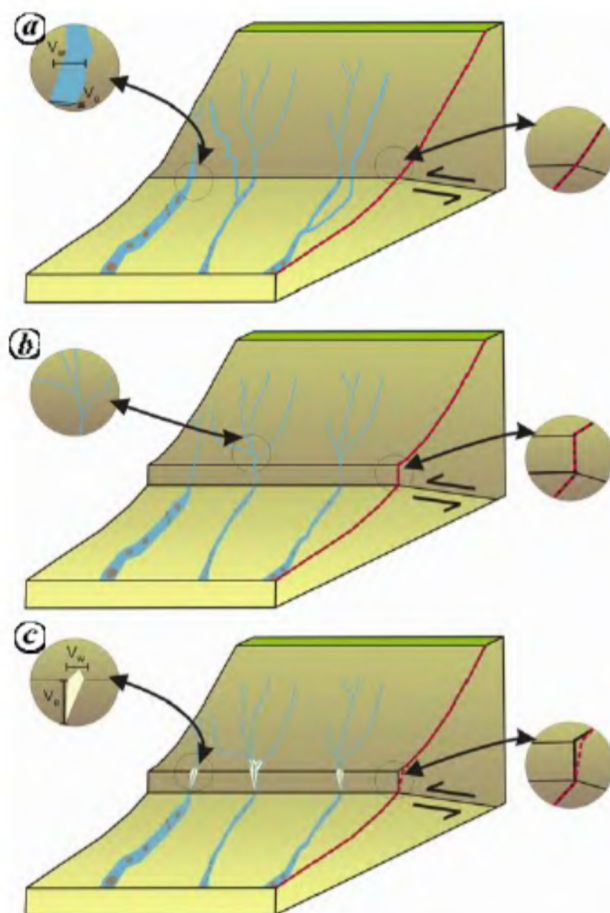


**Figure 4.** Schematic model illustrating the topographic evolution as a result of reactivation of the IFT. The red dashed line shows the topographic slope across the thrust.  $V_w$  and  $V_e$  are valley width and valley elevation respectively. *a*, The inactive thrust is marked by a uniform topographic slope and relatively wide channels. *b*, Tectonic activity (reactivation) along the thrust generates a prominent break in slope along with reorganization of drainage from transverse to longitudinal. *c*, With time, the topographic slope begins to wane (shown by the gentler break in slope of the red line). However, the signatures of tectonic activity may be identified using the narrow valley profiles and sharp break in longitudinal profiles of streams.

The important conclusions of this study are:

- Active tectonic deformation in the hilly terrain of the Nahan Salient caused break in topographic slope, thereby modified the channel slope and stream gradient.
- Active tectonic deformation along the IFT caused an anomalous increase in the SL index at the thrust front.
- In addition, the typical topographic attributes like break in slope, steep valley walls and low values of mountain front sinuosity at the IFT, at a number of places laterally, also corroborate the active tectonic deformation due to the reactivation of IFT. The present approach of using stream profiles appears to be much simpler, easier and faster to locate sites of fault related reactivation. The

interrelationship among the different topographic attributes, thus worked out, is shown Figure 4.

1. Schelling, D. and Arita, K., Thrust tectonics, crustal shortening and the structure of Far-eastern Nepal Himalaya. *Tectonics*, 1991, **10**, 851–862.
2. Delcaillau, B., Carozza, J. M. and Laville, E., Recent fold growth and drainage development: the Janauri and Chandigarh anticlines in Siwalik foothills, NW India. *Geomorphology*, 2006, **76**, 241–256.
3. Yeats, R. S. and Thakur, V. C., Active faulting south of the Himalayan front: establishing a new plate boundary. *Tectonophysics*, 2008, **453**, 63–73.
4. Nakata, T., *Geomorphic History and Crustal Movement of the Foothills of the Himalaya*, Tohoku University, Institute of Geography, 1972, pp. 39–97.
5. Lave, L. and Avouac, J. P., Active folding of fluvial terraces across the Siwalik Hills, Himalayas of central Nepal. *J. Geophys. Res.*, 2000, **105**, 5735–5770.
6. Kumar, S., Wesnousky, S. G., Rockwell, T. K., Briggs, R. W., Thakur, V. C. and Perumal, R. J., Paleoseismic evidence of great surface rupture earthquakes along the Indian Himalaya. *J. Geophys. Res.*, 2006, **111**, B03304.
7. Keller, E. and Pinter, N., *Active Tectonics: Earthquakes, Uplift and Landscape*, Prentice Hall, New Jersey, 2000.
8. Burbank, D. W. and Anderson, R. S., *Tectonic Geomorphology*, Blackwell Publishing, Oxford, 2001.
9. Singh, T. and Virdi, N. S., Tectonic activity classes along the Nahan Thrust (NT) in the NW Sub-Himalaya. *J. Indian Soc. Remote Sensing*, 2007, **35**, 221–230.
10. Singh, T., Sharma, U. and Kumar, R., Soft sediment deformation in Morni area, NW Sub-Himalaya. *Curr. Sci.*, 2007, **93**, 1151–1155.
11. Hack, J. T., Stream profile analysis and stream gradient index. *USGS J. Res.*, 1976, **1**, 421–429.
12. Seeber, L. and Gornitz, V., River profiles along the Himalayan arc as indicators of active tectonics. *Tectonophysics*, 1983, **92**, 335–367.
13. Brookfield, M. E., The evolution of the great river systems of southern Asia during the Cenozoic India–Asia collision: rivers draining southwards. *Geomorphology*, 1998, **22**, 285–312.
14. Chen, Y., Sung, Q. and Cheng, K., Along-strike variations of morphometric features in the western foothills of Taiwan: tectonic implications based on stream gradient and hypsometric analysis. *Geomorphology*, 2003, **56**, 109–137.

**ACKNOWLEDGEMENTS.** We thank the Head, Department of Earth Sciences, Indian Institute of Technology, Roorkee, for providing necessary facilities for the present work. Financial support to T.P.S. from the Department of Science and Technology, New Delhi via grant no. SR/FTP/ES-52/2006 is acknowledged.

Received 3 April 2009; revised accepted 6 November 2009